Published in final edited form as:
Cancer Lett. 2012 August 28; 321(2): 120–127. doi:10.1016/j.canlet.2012.01.014.

Epidermal Growth Factor Receptor-Targeted Photosensitizer Selectively Inhibits EGFR Signaling and Induces Targeted Phototoxicity In Ovarian Cancer Cells

Adnan O. Abu-Yousif[1,†], **Anne C. E. Moor**[1,†,2], **Xiang Zheng**[1], **Mark D. Savellano**[1,3], **Weiping Yu**[1,4], **Pål K. Selbo**[5], and **Tayyaba Hasan**[1,*]

[1]Wellman Center for Photomedicine, Department of Dermatology (Bartlett Hall 314), Massachusetts General Hospital, Harvard Medical School, 40 Blossom Street, Boston, MA 02114, USA

Abstract

Targeted photosensitizer delivery to EGFR expressing cells was achieved in the present study using a high purity, targeted photoimmunoconjugate (PIC). When the PDT agent, benzoporphyin monoacid ring A (BPD) was coupled to an EGFR-targeting antibody (cetuximab), we observed altered cellular localization and selective phototoxicity of EGFR-positive cells, but no phototoxicity of EGFR-negative cells. Cetuximab in the PIC formulation blocked EGF-induced activation of the EGFR and downstream signaling pathways. Our results suggest that photoimmunotargeting is a useful dual strategy for the selective destruction of cancer cells and also exerts the receptor-blocking biological function of the antibody.

Keywords

Ovarian cancer; Photodynamic therapy; cetuximab; Verteporfin; immunoconjugate

1. INTRODUCTION

Ovarian cancer is currently the fifth most lethal cancer among women in the United States [1]. Unfortunately, there is not an established curative treatment option for patients with ovarian cancer. Photodynamic therapy (PDT) is an emerging alternative or complementary treatment option for cancers that are unresectable or refractory to conventional therapies [2; 3; 4]. This strategy has garnered interest because prior treatment with chemotherapy,

*To whom correspondence should be addressed: thasan@partners.org, Telephone: 617-726-6856; Fax: 617-726-8566.
†denotes equal contribution
[2]Current address: photonamic GmbH & Co. KG, Theaterstrasse 6, 22880 Wedel, Germany.
[3]Current address: Surgical Research Laboratory, (HB# 7850), Dartmouth-Hitchcock Medical Center, One Medical Center Drive, Lebanon, NH 03756, USA.
[4]Current address: Department of Radiology, Emory University, Atlanta, GA 30322
[5]Current address: Department of Radiation Biology, Institute for Cancer Research, Norwegian Radium Hospital, Oslo University Hospital, Norway

CONFLICT OF INTEREST STATEMENT
The authors declare that there are no conflicts of interest.

ionizing radiation, or surgery does not preclude patients from receiving PDT [5], and PDT treatment does not interfere with the pharmacokinetic and pharmacodynamic properties of other anti-neoplastic agents [6]. Furthermore, PDT has been shown to sensitize cancer cells to chemotherapeutic and biologic agents [7] and directly stimulates cell death by bypassing apoptotic machinery [8; 9] making it an attractive approach to treat malignancies with poor prognosis such as ovarian cancer.

The principle mode of action for photodynamic therapy is through the generation of active molecular species created by excitation of a nontoxic chemical (known as a photosensitizer), thus producing localized toxicity [10]. PDT has yet to advance beyond clinical trials for ovarian cancer, where median patient survival for those treated with the first generation photosensitizer, Photofrin®, exceeded expectations for patients with pleural and peritoneal disease treatment compared to standard therapeutic regimens [11; 12]. While these trials and others have demonstrated the utility of PDT for intraperitoneal cancers, dose limiting toxicities such as bowel perforations [13] and tissue damage to the serosal surfaces in the peritoneal cavity [11] have been observed. The use of sub-optimal treatment parameters including a lack of photosensitizer tumor selectivity has limited therapeutic response, but these trials illustrate the promise of the technology [11; 12; 13; 14].

One strategy to improve treatment response is to combine PDT with non-overlapping therapeutic modalities. The epidermal growth factor receptor (EGFR) is an attractive target, with over-expression being correlated to poor prognosis in many cancers including ovarian, colorectal carcinoma, head and neck, lung, and pancreatic cancer among others [15]. Monoclonal antibodies (mAb) targeting the EGFR, including the chimeric immunoglobulin G1 (IgG1) anti-EGFR mAb cetuximab (C225) have proven modestly effective for managing some of these diseases alone and somewhat more effective in combination with mechanistically non-overlapping therapeutic modalities [16; 17]. We have demonstrated that cetuximab in combination with PDT resulted in synergistic reduction in tumor burden and increased overall survival in a preclinical model of disseminated ovarian carcinamatosis [18]. This work has helped form the basis of large animal studies in preparation for clinical trials [19], but the approach of using cetuximab and PDT in two steps still lacks the level of selectivity desired for optimal treatment.

Motivated by these encouraging findings, we have developed a high-purity, functional photosensitizer immunoconjugate (PIC) capable of simultaneous delivery of the long wavelength absorbing photosensitizer benzoporphyrin derivative monoacid A (BPD) and the EGFR-targeting antibody, cetuximab [20; 21]. The strategy of photoimmunotargeting (PIT) first reported by Mew et al in the 1980s [22], and further developed by many groups including ours, showed promise as an approach for treating diseases with complex dissemination such as ovarian cancer where mitigating damage to healthy tissues is essential [21; 23]. This strategy allows for simultaneous delivery of two non-overlapping therapies with the likelihood for greater therapeutic benefit than with either agent alone. It also provides the potential for lower doses of each agent thus lowering associated toxicities. Unfortunately, early PIC formulations were often confounded by aggregation and the presence of free photosensitizer impurities making interpretation of previous work, including our own, challenging. To overcome aggregation we conjugated cetuximab with a 10 kDa two-branched polyethylene glycol (PEG) and minimized the presence of free photosensitizer by optimizing the photosensitizer:antibody ratio [21].

In the present study, we build on previous work describing the photophysical and biological properties of the PIC [20; 21] and investigate the effect of photoimmunotargeting on the key molecules along the EGFR signaling pathway. We demonstrate that cetuximab retains EGFR targeting capacity and biological activity following conjugation with BPD.

Furthermore, we show that conjugation of BPD to cetuximab alters the *in vitro* subcellular localization of BPD from the mitochondria [24] to the lysosomes, which corresponds with the subcellular localization observed for free cetuximab [25]. The presence of cetuximab as a single agent or as part of the PIC similarly inhibited EGF-induced phosphorylation of EGFR and two downstream molecules, Akt and MAPK/ERK that are part of the pathways involved in growth arrest chemosensitivity and angiogenic effects. Collectively, these data show that our PIC is functional at targeting and inhibiting the biological function of the EGFR and that simultaneous administration of a PDT agent and EGFR inhibitor, as enabled by this method, may offer some advantage over separate administration.

2. MATERIALS AND METHODS

Materials

Cetuximab was provided by ImClone, Inc. (New York, NY), in a 2 mg/ml stock solution. BPD was a gift from QLT Inc. (Vancouver, BC, Canada) and kept at 4 °C in the dark. EGF was obtained from R & D Systems Inc. (Minneapolis, MN). All other reagents were of analytical grade.

Cell lines—NIH:OVCAR-5 cells (OVCAR-5) were obtained from Thomas Hamilton, Fox Chase Cancer Institute (Philadelphia, PA) and maintained in RPMI-1640 (Mediatech Inc., Herndon, VA) supplemented with 10% heat-inactivated fetal bovine serum (FBS, GIBCO Life Technologies, Grand Island, NY), 100 U/ml penicillin, and 100 μg/ml streptomycin. CHO cells stably transfected with EGFR full-length receptor (CHO-EGFR) or HER2 (CHO-HER2) were grown in Ham's F12 selective media (containing 0.8 μg/ml G418/neomycin) with 10% FBS. The parent cell line (CHO-WT) was maintained in non-selective Ham's F12 complete media. These cells were kindly provided by Dr. T. Heitner [26], Department of Anesthesiology, UCSF, San Francisco, CA.

Preparation of the BPD-cetuximab conjugate—Conjugates of BPD and cetuximab were prepared by modifying a previous protocol [20; 21]. Briefly, the *N*-hydroxysuccinimide ester of BPD was reacted with cetuximab, which had previously been PEGylated. The resulting PIC was purified on a Sephadex G-50 column (Amersham Pharmacia Biotech Inc., Piscataway, NJ) or a Zeba spin desalting column (ThermoScientific Rockford, IL). The purity of PIC was confirmed using gel electrophoresis (Ready Gel 5% Tris-HCl, Bio-Rad Laboratories). The molar ratio of photosensitizer (PS) to mAb was measured using a BCA protein assay (Pierce, Rockford, IL) to determine protein content and absorbance spectroscopy at 690 nm to determine PS content. Typically, the conjugates used in this study had a PS:mAb molar ratio of 7:1.

Subcellular localization—The subcellular localization of BPD, PIC and cetuximab were established by confocal microscopy as described in detail previously [27; 28]. In order to visualize cetuximab, the antibody was labeled using an antibody labeling kit as directed by the manufacturer (Invitrogen). Cells were grown on coverslips, incubated for 40 hours with cetuximab-Alexa488, cetuximab-Alexa647, BPD or BPD-cetuximab, fixed in 4% formalin for 15 minutes, washed in PBS, and then mounted on microscope slides using SlowFade Gold Antifade reagent (Invitrogen, Carlsbad, CA). Confocal laser fluorescence microscopy was carried out using an Olympus FV1000 hyperspectral laser scanning confocal and multiphoton microscope. For this study, a 0.8 NA 40X LUMPLFL objective was used. Co-localization studies were performed by co-incubating the cells for the final 45 to 60 minutes of the total 40 hour incubation period with either 100 nM LysoTracker® Red DND-99 for staining of lysosomes or 100 nM MitoTracker® Orange CM-H2TMRos for staining of mitochondria, respectively (Invitrogen). For presentation purposes, each organelle stain has

been pseudocolored green while the agents of interest (BPD, PIC, and cetuximab) have been pseudocolored red. Colocalization was determined using the Matlab programming toolkit (Mathworks) and the open-source LOCI tools. Briefly, raw image data was passed through to create a mask for organelle fluorescence that was used to determine colocalization with the fluorophore of interest (BPD or cetuximab).

Photosensitizer binding—Binding of BPD and BPD-cetuximab conjugate in OVCAR-5, CHO-WT, CHO-EGFR, and CHO-HER2 cells was measured as previously described [27]. Briefly, cells were incubated for 15 hours with either BPD or the PIC and, after washing, solubilized in 1% SDS/0.1 M NaOH or incubated with Solvable (Perkin Elmer, Waltham, Ma) for 2 hours at 37°C. Fluorescence was measured, compared to standards prepared from known concentrations of BPD or PIC, and calculated as μmol of PS per mg cell protein. To assess the targeting ability of the PIC, ratios of PIC-associated BPD binding to free BPD binding were calculated; this ratio represents the selectivity conferred by the PIC.

Photodynamic Therapy—A solid-state diode laser (BWF 690-1, B&W TEK, Newark, DE) delivered monochromatic light (690 +/− 5 nm), which overlaps closely with the absorption maximum of BPD (690 nm). This light was focused to a spot of 3.5 cm diameter with an irradiance of 40 mW/cm^2. PDT using BPD or BPD-cetuximab PIC was performed as previously described [29]. OVCAR-5 or CHO cells were plated in 35 mm dishes, incubated with BPD or PIC for 15 hours, and subsequently illuminated with either 0.5 (BPD-PDT) or 20 J/cm^2 (PIC-PDT) of light. MTT assay was performed or cell lysates were prepared for Western blotting 24 hours after PDT. In one set of experiments, cells underwent a single wash step with fresh culture medium before illumination in order to remove any loosely bound BPD or BPD-cetuximab conjugate.

Cytotoxicity—The 3-(4,5-dimethylthiazol-2-yl)-2,5-diphenyltetrazolium bromide (MTT) assay, which measures mitochondrial dehydrogenase activity, was used. Cells were incubated with 0.5 mg/ml MTT for 1 hour to measure its reduction by mitochondrial dehydrogenases as recommended by the manufacturer (Sigma).

Western blotting—In order to examine the EGF-induced phosphorylation of the EGFR as well as phosphorylation of two associated downstream signaling molecules following PDT, OVCAR-5 cells were incubated with cetuximab or PS in the form of BPD or BPD-cetuximab PIC. Samples were in duplicate for each treatment group. Samples incubated with PS were exposed to no light or a light dose sufficient to induce ~50% cytotoxicity. The concentration of BPD in the PIC was 250 nM BPD equivalent. The concentration of cetuximab (approximately 37 nM), corresponded to the amount of cetuximab present in the PIC (BPD: cetuximab • 7:1). 24 hours post treatment one of the plates was incubated with 10 ng/ml EGF for 15 minutes to stimulate EGFR activity prior to harvesting whole cell lysates for Western Blotting. Thus, there were a total of 12 different treatment conditions. After protein determination by a modified Lowry assay (Biorad, Hercules, CA), the lysates were run on SDS-PAGE, transferred to a PVDF membrane (Immobilon-P, Millipore, Bedford, MA), and probed with the first antibody. The following antibodies were purchased from Cell Signaling (Danvers, MA): anti-EGFR tyr 1068 (Product ID: 2234), anti-phospho-Akt ser 473 (Product ID: 4058), Anti-Akt (Product ID: 9272), anti- β-actin (Product ID: 4970), Phospho-p44/42 MAPK (Erk1/2) (Product ID: 4377), p44/42 MAPK (Erk1/2) (Product ID: 4695), and Anti-rabbit IgG, HRP-linked Antibody (Product ID: 7074). Anti-EGFR was obtained from Millipore (Product ID: 06-847, Billerica, MA). Protein bands were detected using the SuperSignal West Femto Maximum Sensitivity Substrate enhanced chemiluminescence (ECL) kit (Thermo Scientific, Rockford, IL) on a Kodak Image station

4000R equipped with molecular imaging software to perform densitometric analysis. Signal intensities were normalized to actin signals. Data were normalized relative to untreated controls.

Statistical Analysis

A paired, two-tailed Student's t-test was used to compare the mean viability of samples that were left untreated (NT-no treatment control) or treated with different doses of photodynamic therapy. Values were determined by evaluating response in three or more independent experiments with samples collected in triplicate for each experiment. Comparisons of viability were made in the same cell line; biological variation among different cell lines hinders comparison between cell lines. Co-localization of BPD and BPD-cetuximab with MitoTracker and LysoTracker was assessed using a custom MatLab algorithm that assigns a numerical value for the percent of photosensitizer that is present in a particular cellular compartment in confocal image stacks taken using an Olympus FV1000. Statistical comparisons between the cellular compartmentalization in a given cell line was made by taking at least four fields per dish in at least three independent experiments resulting in over one hundred cells analyzed per condition. Colocalization percentages were then compared using one-way ANOVA with a Tukey's multiple comparison test.

3. RESULTS

BPD-cetuximab selectively binds to EGFR-positive cells

The EGFR-targeting capacity of cetuximab following conjugation with BPD was assessed in EGFR-negative (CHO cells transfected with control vector or HER2 vector) and EGFR-positive (CHO cells transfected with EGFR and the ovarian cancer cell line, OVCAR-5) cells. Whole cell lysates were harvested for Western blot analysis of EGFR status (Figure 1A). EGFR expression in EGFR-negative cell lines was negligible compared to the EGFR-positive cell lines used.

Quantitative binding of free BPD and the PIC (BPD equivalents) to EGFR-positive and EGFR-negative cell lines was established by fluorescence spectroscopy of the lysed cells and expressed as the ratio of cell-bound PIC content to cell-bound free BPD content (Figure 1B). The EGFR-negative cell lines evaluated (CHO cells and CHO cells transfected with an EGFR family member, HER2) exhibited very limited binding of BPD-cetuximab (ratios of PIC binding to free BPD binding of 0.02 and 0.11, respectively). In CHO-EGFR cells, the BPD-cetuximab binding was slightly higher than that of free BPD (a ratio of 1.26). In OVCAR-5 cells, the ratio of PIC to BPD binding was significantly greater than in CHO cells transfected with either the control vector or HER2 (Student's T-test $p < 0.005$). While not statistically significant, the PIC:free BPD binding ratio was lower in the OVCAR-5 cells than in the CHO-EGFR cell line, which appears to reflect the fact that EGFR expression is somewhat lower in OVCAR-5 cells compared to CHO-EGFR cells. By comparison to cells that do not express the receptor, CHO-EGFR and OVCAR-5 cells selectively bind to and/or take up the PIC relative to free BPD. Importantly, these results demonstrate the specificity of PIC binding to EGFR-expressing cells and minimal binding to HER2 expressing cells (HER2 is an EGFR-family member but distinct from the EGFR). This differential binding to EGFR-expressing cells is one of the important determinants of selectivity of the PIC-based approach.

Conjugation of BPD to cetuximab alters cellular localization

The preferential interaction of the PIC with target cells was established by cellular localization of the PICs using confocal laser microscopy. One of the benefits to coupling a PS to a targeting agent instead of a traditional cytotoxic therapeutic is that one can visualize

the fluorescence to determine the accumulation of the PS in cells and tissues. Without conjugation to a targeting moiety, BPD lacks selectivity and accumulates in both EGFR-positive and EGFR-negative cell lines (Figure 2A and B). Conjugation of BPD to cetuximab results in EGFR selective binding, as demonstrated by the BPD fluorescence observed in the CHO-EGFR cells (Figure 2D) and lack of BPD fluorescence in EGFR-negative cells (CHO-HER2; Figure 2E).

The change in staining pattern of BPD fluorescence led us to investigate the cellular localization of BPD-cetuximab in the EGFR-expressing OVCAR-5 cell line. Previous studies have reported that BPD fluorescence co-localized with MitoTracker [27; 28]; however, we observed a rather heterogenous pattern of BPD fluorescence. To address this we incubated cells with equivalent BPD concentrations of BPD and PIC and co-stained with fluorescent dyes that label the mitochondria (MitoTracker) and lysosomes (LysoTracker). Using a custom image analysis routine to batch process confocal image data of 10, 1.0-μm step z-planes per field we were able to determine the percentage of total BPD fluorescence that co-localized with MitoTracker or LysoTracker (pseudocolored green in Figure 3). In each of the figures BPD (as a single agent or formulated as the PIC) has been pseudocolored red. As shown in Figure 3B the PIC increased BPD accumulation in the lysosomal compartment as a shift in co-localization with LysoTracker (Figure 3B and 3D) from 10% +/− 1% to 51% +/− 4.5% was observed. We performed a one way ANOVA with Tukey's Multiple comparison test to compare the percentage of BPD with the percentage of PIC that co-localized with mitochondrial and lysosomal dyes. [Lyso: $P < 0.05$, Mito: $P > 0.05$]. In addition, we found that the localization of cetuximab (pseudocolored red) in the lysosomes is not significantly different from that of the PIC formulation (Figure 3B and 3D). Collectively, these results suggest that the PIC construct was reliable in that its binding to cells is dependent on the expression level of EGFR in target cells, and that EGFR positive cells internalize the PIC formulation through vesicle-mediated transport into lysosomes, which has been noted for cetuximab in the absence of conjugation [25]. Accumulation of BPD associated with the PIC in the lysosomes could explain observed differences in photosensitization efficacy between free BPD and the PIC.

PIC Phototoxicity is enhanced in EGFR expressing cells

The specific binding of the PIC (BPD concentration of 250 nM) translated into significantly ($p<0.05$) higher phototoxicity in the CHO-EGFR cells compared to the CHO-HER2 (EGFR negative) cells 24 hours after illumination (Figure 4). At a light dose of 20 J/cm^2, the cell viability for CHO-EGFR cells treated with BPD-cetuximab PIC decreased to less than 20% of NT control, while the viability of the CHO-HER2 cells treated with BPD-cetuximab PIC was about 60%. To demonstrate the selective binding of the PIC under *in vitro* conditions that represents a closer approximation to the *in vivo* situation where cells are washed many times over by blood and lymphatic fluids we included an additional wash step to remove excess BPD-cetuximab that was not bound to the EGFR prior to illumination. Under these conditions, the phototoxic effects of BPD-PDT alone or in combination with cetuximab were not altered by the additional wash step. However, the specificity of the PIC-induced phototoxic effects was more pronounced. By washing the EGFR-negative CHO-HER2 cells the effects of illumination was negligible, with a cell viability of 99%. Therefore, phototoxicity observed in CHO-HER2 cells in the absence of washing was likely due to non-specific PDT. However, when the CHO-EGFR and EGFR-expressing OVCAR-5 cell lines were washed prior to illumination the PIC-induced phototoxicity was comparable to that observed in cells that were not washed prior to irradiation. The absence of the "wash" on target cells may be attributed to the internalization of the PIC, suggesting that the phototoxicity for these cells is predominantly due to selective PIC internalization rather than non-specific sticking of the PIC on the cell surface. It is also possible that the level of

stickiness of the two cell lines is different. One may speculate that the additional "wash-step" protocol could explain the higher *in vivo* specificity previously noted for PIC-PDT [30; 31]. In contrast, free BPD caused significant decrease in cell viability for both CHO-EGFR and CHO-HER2 cells, as measured with the MTT assay 24 hours after exposure to red light. All cell lines evaluated showed less than 15% viability at a light dose of 2 J/cm^2 (data not shown). The above results established that the BPD-cetuximab PIC was specific for the EGFR-transfected CHO cells and the EGFR-expressing ovarian cancer cell line OVCAR-5.

Photoimmunotargeting affects EGFR phosphorylation and its downstream signaling

In the next step, we investigated whether the biologic activity of cetuximab was retained following chemical conjugation with BPD. Specifically, we assessed the ability of EGF to induce activation of the EGFR signaling cascade by evaluating phosphorylation of the EGFR and two downstream signaling molecules (Akt and MAPK/ERK) in OVCAR-5 cells treated with BPD-PDT, cetuximab alone, PIC alone, or PIC-PDT. Cells were exposed to the LD_{50} for BPD-PDT or PIC-PDT as described above, and then 10 ng/ml EGF was added to the media at 37°C during the last fifteen minutes of the 24 hour incubation in order to stimulate the EGFR signaling cascade. In the absence of cetuximab, activation of the EGFR signaling pathway was observed, as can be seen by the increased phosphorylation of the EGFR, Akt (Figure 5A) and MAPK/ERK (Figure 5B). However, in the presence of cetuximab (either as mAb alone or in the BPD-cetuximab PIC), activation of the EGFR, Akt, (Figure 5A) and MAPK/ERK (Figure 5B) was inhibited even in samples treated with PDT. Densitometric analysis of the individual bands relative to β-actin and total EGFR show that BPD-PDT treated samples were more responsive to EGF stimulation of EGFR activity than control cells; for BPD-PDT treated samples, the addition of EGF stimulated phosphorylation of EGFR to 180% of that observed in the no treatment control (Figure 5A). Similarly, EGF-induced phosphorylation of the downstream signaling molecules Akt and MAPK/ERK after BPD-PDT was increased by 190% and 235% compared to the no treatment control (Figure 5A and B). These results suggest that PDT alone may sensitize the cells to EGFR stimulation and subsequent Akt phosphorylation (Figure 5A). In contrast, the cetuximab component of the PIC effectively inhibited the sensitization of EGFR signaling as demonstrated by the reduced capacity of EGF to induce EGFR, Akt, and MAPK/ERK phosphorylation (Figure 5A and B).

4. DISCUSSION

Development of therapeutics that target mediators of cell proliferation and survival, such as EGFR and its family members, is a major quest in cancer research. For example, cetuximab mitigates proliferative signals initiated by EGFR signaling and has been licensed for the treatment of colorectal cancer [32], with subsequent approvals for use in non-small cell lung cancer and squamous cell carcinoma of head and neck cancer [15]. It is also used investigationally or on compassionate grounds for other cancers [33; 34]. Subsequent studies have demonstrated that when cetuximab is used in combination with non-overlapping therapies, overall survival increases for patients with colorectal cancer [35] and squamous-cell head and neck cancer [36]. In keeping with this theme, many preclinical investigations have demonstrated that growth factor signaling inhibition in combination with PDT offers improved therapeutic outcome compared to either approach as a monotherapy [18; 37; 38]. While these strategies have shown promise, they fail to address the pressing issue of photosensitizer tumor selectivity that has been described as a limiting factor in PDT-based clinical trials for intraperitoneal cancers [11; 12].

To address the issue of selectivity, many groups, including ours, are investigating ways to improve selective delivery of drugs and photosensitizers through chemical conjugation to

monoclonal antibodies and other targeting moieties [20; 21; 29; 39]. The current study demonstrated that when cetuximab is conjugated to BPD, its anti-EGFR activity and phototoxic abilities are retained, thus providing a combination therapy with a single agent administration. Simultaneous delivery of multiple agents overcomes limitations imposed by sequential administration of biological therapies such as bevacizumab (Avastin) that causes blood vessel remodeling [40]. The observations made in the present study demonstrate that conjugation of BPD to cetuximab results in exquisite targeted delivery of the PIC to EGFR-expressing cells. The BPD-cetuximab PIC selectively binds to and induces phototoxicity in EGFR-positive cell lines while largely sparing EGFR-negative cells, including a HER2 expressing cell line (HER2 is a related EGFR family member but is distinctly different from the EGFR). Moreover, when an additional wash step prior to irradiation was incorporated to more closely mimic in vivo administration where blood and lymphatic fluids wash away agents that are not tightly bound to their targets, PIC phototoxic selectivity was further improved. The additional "wash-step" could explain the higher *in vivo* specificity previously noted for PIC-PDT [30; 31]. Conjugation of BPD to cetuximab also altered the localization of BPD from the mitochondria to the lysosomes, suggesting that the PIC follows vesicle-mediated transport, as has been noted for cetuximab [25]. Localization of the PIC to lysosomes, which are less photosensitive with respect to apoptosis than the mitochondria [41; 42], may account for the observed decrease in phototoxic efficacy of the PIC relative to the free PS. Nonetheless, the decreased phototoxic efficacy of the PIC should be surmountable by increasing the administered light dose.

Our observations regarding the inhibition of EGFR, Akt, and MAPK/ERK phosphorylation by cetuximab alone and the PIC appear to corroborate the observations of enhanced effectiveness of cytotoxic therapies in the presence of cetuximab, as observed in both preclinical and clinical studies [15]. The biological activity of the cetuximab component of the PIC was demonstrated by the inhibition of EGF-induced phosphorylation of EGFR and downstream signaling molecules (Figure 5). Both the RAS-MEKK-MAPK/ERK and the PI3K-PDK-Akt pathways are involved in proliferation of cells, either directly or via the inhibition of apoptosis. After activation by the RAS-MEKK-MAPK/ERK pathway, MAPK/ERK can translocate to the nucleus, where it can activate transcription factors that are involved in mitogenesis [43]. Akt is involved in regulation of the cell cycle regulating protein, cyclin D, and upon activation of Akt, cells can enter the cell cycle [44]. The receptor tyrosine kinase inhibition activity of cetuximab blocks subsequent receptor phosphorylation, thereby inducing cell cycle arrest through induction of the tumor suppressor protein p27 [45; 46]. An important target of both MAPK/ERK and Akt is BAD, which upon phosphorylation by both MAPK/ERK and Akt, can release the anti-apoptotic molecule Bcl-2, thereby conveying a survival signal for the cells [47; 48]. BAD phosphorylation has been implicated in the occurrence of platinum resistance in ovarian cancer cells. Cisplatin induces the PI3K-Akt-BAD cascade and this pathway might be involved in the induction of DNA repair. Consequently, inhibition of either the PI3K pathway or the MEK-MAPK/ERK pathway, resulting in inhibition of BAD phosphorylation, sensitized cells to cisplatin treatment [49]. Oxidative stress responses initiated following PDT can lead to the degradation of the EGFR immediately following PDT [38; 50]; however, in the present study we demonstrate that PDT sensitizes EGFR expressing OVCAR-5 cells to EGF-induced phosphorylation of EGFR and downstream signaling 24 hours following PDT (Figure 5). These phosphorylation events were inhibited by cetuximab alone or as part of the PIC. Consistent with these observations, the cetuximab in the PIC is still functional and maintains selectivity without any significant mistargeting even within the same EGFR family (e.g., HER2), as shown in Figure 4.

This PIC-based strategy allows for simultaneous administration of multiple agents in a single dose and offers targeted delivery of the cytotoxic compound to the tissue of interest.

Previous coupling efforts targeted conventional tumor-associated antigens that are shed into the circulation from tumor cells, e.g., the CA125 antigen [23; 51]. More recent efforts have focused on targeting antigens that are highly expressed in cancer cells such as the EGFR or HER2 [20; 52; 53; 54]. EGFR-targeted delivery of photosensitizers could have broad clinical implications, given that many cancers overexpress EGFR [15]. The potential advantages are twofold: 1) Improved selectivity should reduce off-target effects of PDT in healthy tissues allowing application of PDT to complex sites in a broad range of cancers, and 2) improved contrast when using BPD fluorescence to guide treatment planning [55]. The results presented in this study are encouraging and have inspired us to investigate the potential of BPD-cetuximab PDT as a dual purpose treatment and diagnostic imaging agent in a murine model of disseminated ovarian cancer, which might also be applicable to other diseases as well. Photosensitizers are currently used to detect bladder and to guide surgical resection of cancer [56], and have become especially valuable in guiding surgical resection and treatment of malignant gliomas [57; 58]. Intraperitoneal PDT using the first generation photosensitizer Photofrin resulted in prolonged disease-free survival, and a median survival of 21 months despite the advanced stage of disease found in the patients [12]. Bowel perforation and fistula formation were some of the major dose-limiting toxicities noted in previous clinical trials of intraperitoneal disease [13]. These complications along with prolonged skin photosensitivity are primarily the result of non-specific accumulation of the photosensitizer, Photofrin. Despite these limitations, encouraging results from previous trials from the pioneering work at the National Cancer Institute [13] and groups at the University of Pennsylvania [11; 12; 14] suggest that PDT could be an effective modality for treating ovarian cancer if the challenge of non-specific photosensitizer accumulation can be overcome. Another potential advantage of PDT is that reports suggest it is effective against cancer cells that show resistance to standard chemo and radiation therapies [7]. Therefore, a more selective PDT agent that has a dual targeting capacity, such as in the PIC described in this study, enhances the potential of the PIC therapeutic approach significantly. The 40 hour incubation noted in this study for effective cell killing is a reflection of a mixture of optimal selectivity and cellular uptake. Prior work with PICs, both by us others [21; 39; 54; 59], has shown that this delay between PIC and light administration does not result in skin phototoxicity, although this issue requires further study. As with any targeted therapy, the efficacy will be limited by the degree of expression and the functionality of the target. The approach developed here could be used for other targets. With the availability of bispecific antibodies and advances in nanotechnology, therapies could be directed to several targets simultaneously. These approaches are under investigation in several laboratories including ours. Overall, our data show that the approach is promising and merits further investigation in vivo in appropriate animal models to establish its potential utility for the treatment of advanced ovarian cancer.

Acknowledgments

This study was supported by the National Institutes of Health grant RO1AR40352, 5R01CA160998, PO1CA84203, a grant from the Massachusetts Department of Public Health, (34081126112), and the Whitaker Foundation (MS). We thank Drs. Tara Heitner and James Marks (UCSF) for providing the transfected cell lines, and Drs. Jonathan P. Celli, Imran Rizvi, Mr. Nathaniel Sznycer-Taub, and Ms Divya Errabelli for superb technical advice.

REFERENCES

1. Jemal A, Siegel R, Xu J, Ward E. Cancer statistics, 2010. CA Cancer J Clin. 60:277–300. [PubMed: 20610543]
2. Allison RR, Zervos E, Sibata CH. Cholangiocarcinoma: an emerging indication for photodynamic therapy. Photodiagnosis Photodyn Ther. 2009; 6:84–92. [PubMed: 19683207]
3. Fan BG, Andren-Sandberg A. Photodynamic therapy for pancreatic cancer. Pancreas. 2007; 34:385–389. [PubMed: 17446835]

4. Ross P Jr. Grecula J, Bekaii-Saab T, Villalona-Calero M, Otterson G, Magro C. Incorporation of photodynamic therapy as an induction modality in non-small cell lung cancer. Lasers Surg Med. 2006; 38:881–889. [PubMed: 17115382]
5. Biel MA. Photodynamic therapy of head and neck cancers. Methods Mol Biol. 2011; 635:281–293. [PubMed: 20552353]
6. Ortel B, Shea CR, Calzavara-Pinton P. Molecular mechanisms of photodynamic therapy. Front Biosci. 2009; 14:4157–4172. [PubMed: 19273342]
7. Duska LR, Hamblin MR, Miller JL, Hasan T. Combination photoimmunotherapy and cisplatin: effects on human ovarian cancer ex vivo. J Natl Cancer Inst. 1999; 91:1557–1563. [PubMed: 10491432]
8. Kessel D. Death pathways associated with photodynamic therapy. Med Laser Appl. 2006; 21:219–224. [PubMed: 19890442]
9. Kessel D. Promotion of PDT efficacy by a Bcl-2 antagonist. Photochem Photobiol. 2008; 84:809–814. [PubMed: 18179619]
10. Hasan, T.; Ortel, B.; Solban, N.; Pogue, B. Photodynamic therapy of cancer. Hamilton, Ontario: B.C. Decker Inc; 2006.
11. Hahn SM, Fraker DL, Mick R, Metz J, Busch TM, Smith D, Zhu T, Rodriguez C, Dimofte A, Spitz F, Putt M, Rubin SC, Menon C, Wang HW, Shin D, Yodh A, Glatstein E. A phase II trial of intraperitoneal photodynamic therapy for patients with peritoneal carcinomatosis and sarcomatosis. Clin Cancer Res. 2006; 12:2517–2525. [PubMed: 16638861]
12. Hendren SK, Hahn SM, Spitz FR, Bauer TW, Rubin SC, Zhu T, Glatstein E, Fraker DL. Phase II trial of debulking surgery and photodynamic therapy for disseminated intraperitoneal tumors. Ann Surg Oncol. 2001; 8:65–71. [PubMed: 11206227]
13. DeLaney TF, Sindelar WF, Tochner Z, Smith PD, Friauf WS, Thomas G, Dachowski L, Cole JW, Steinberg SM, Glatstein E. Phase I study of debulking surgery and photodynamic therapy for disseminated intraperitoneal tumors. Int J Radiat Oncol Biol Phys. 1993; 25:445–457. [PubMed: 8436523]
14. Wilson JJ, Jones H, Burock M, Smith D, Fraker DL, Metz J, Glatstein E, Hahn SM. Patterns of recurrence in patients treated with photodynamic therapy for intraperitoneal carcinomatosis and sarcomatosis. Int J Oncol. 2004; 24:711–717. [PubMed: 14767557]
15. Mendelsohn J, Baselga J. Epidermal growth factor receptor targeting in cancer. Semin Oncol. 2006; 33:369–385. [PubMed: 16890793]
16. Capdevila J, Elez E, Macarulla T, Ramos FJ, Ruiz-Echarri M, Tabernero J. Anti-epidermal growth factor receptor monoclonal antibodies in cancer treatment. Cancer Treat Rev. 2009; 35:354–363. [PubMed: 19269105]
17. Martinez-Carpio PA, Trelles MA. The role of epidermal growth factor receptor in photodynamic therapy: a review of the literature and proposal for future investigation. Lasers Med Sci. 2010; 25:767–771. [PubMed: 20535519]
18. del Carmen MG, Rizvi I, Chang Y, Moor AC, Oliva E, Sherwood M, Pogue B, Hasan T. Synergism of epidermal growth factor receptor-targeted immunotherapy with photodynamic treatment of ovarian cancer in vivo. J Natl Cancer Inst. 2005; 97:1516–1524. [PubMed: 16234565]
19. Lewis, R.; Schuman, L.; Mickler, M.; Durham, A.; Evans, S.; Glatstein, E.; Hahn, S.; Fraker, D.; Cengel, K. RI: 35th American Society for Photobiology Providence; 2010. Preclinical Evaluation of Cetuximab and Benzoporphyrin Derivative-Mediated Intraperitoneal Photodynamic Therapy in a Canine Model.
20. Savellano MD, Hasan T. Targeting cells that overexpress the epidermal growth factor receptor with polyethylene glycolated BPD verteporfin photosensitizer immunoconjugates. Photochemistry and photobiology. 2003; 77:431–439. [PubMed: 12733655]
21. Savellano MD, Hasan T. Photochemical targeting of epidermal growth factor receptor: a mechanistic study. Clin Cancer Res. 2005; 11:1658–1668. [PubMed: 15746071]
22. Mew D, Wat CK, Towers GH, Levy JG. Photoimmunotherapy: treatment of animal tumors with tumor-specific monoclonal antibody-hematoporphyrin conjugates. J Immunol. 1983; 130:1473–1477. [PubMed: 6185591]

23. Duska LR, Hamblin MR, Bamberg MP, Hasan T. Biodistribution of charged F(ab')2 photoimmunoconjugates in a xenograft model of ovarian cancer. Br J Cancer. 1997; 75:837–844. [PubMed: 9062404]
24. Peng TI, Chang CJ, Guo MJ, Wang YH, Yu JS, Wu HY, Jou MJ. Mitochondrion-targeted photosensitizer enhances the photodynamic effect-induced mitochondrial dysfunction and apoptosis. Ann N Y Acad Sci. 2005; 1042:419–428. [PubMed: 15965088]
25. Sunada H, Magun BE, Mendelsohn J, MacLeod CL. Monoclonal antibody against epidermal growth factor receptor is internalized without stimulating receptor phosphorylation. Proc Natl Acad Sci U S A. 1986; 83:3825–3829. [PubMed: 2424012]
26. Heitner T, Moor A, Garrison JL, Marks C, Hasan T, Marks JD. Selection of cell binding and internalizing epidermal growth factor receptor antibodies from a phage display library. J Immunol Methods. 2001; 248:17–30. [PubMed: 11223066]
27. Pogue BW, Ortel B, Chen N, Redmond RW, Hasan T. A photobiological and photophysical-based study of phototoxicity of two chlorins. Cancer Res. 2001; 61:717–724. [PubMed: 11212274]
28. Runnels JM, Chen N, Ortel B, Kato D, Hasan T. BPD-MA-mediated photosensitization in vitro and in vivo: cellular adhesion and beta1 integrin expression in ovarian cancer cells. Br J Cancer. 1999; 80:946–953. [PubMed: 10362101]
29. Savellano MD, Pogue BW, Hoopes PJ, Vitetta ES, Paulsen KD. Multiepitope HER2 targeting enhances photoimmunotherapy of HER2-overexpressing cancer cells with pyropheophorbide-a immunoconjugates. Cancer Res. 2005; 65:6371–6379. [PubMed: 16024640]
30. Goff BA, Bamberg M, Hasan T. Photoimmunotherapy of human ovarian carcinoma cells ex vivo. Cancer Res. 1991; 51:4762–4767. [PubMed: 1716512]
31. Goff BA, Hermanto U, Rumbaugh J, Blake J, Bamberg M, Hasan T. Photoimmunotherapy and biodistribution with an OC125-chlorin immunoconjugate in an in vivo murine ovarian cancer model. Br J Cancer. 1994; 70:474–480. [PubMed: 8080733]
32. Adams GP, Weiner LM. Monoclonal antibody therapy of cancer. Nat Biotechnol. 2005; 23:1147–1157. [PubMed: 16151408]
33. Lukan N, Strobel P, Willer A, Kripp M, Dinter D, Mai S, Hochhaus A, Hofheinz RD. Cetuximab-based treatment of metastatic anal cancer: correlation of response with KRAS mutational status. Oncology. 2009; 77:293–299. [PubMed: 19923868]
34. Bernier J, Bentzen SM, Vermorken JB. Molecular therapy in head and neck oncology. Nat Rev Clin Oncol. 2009; 6:266–277. [PubMed: 19390553]
35. Cunningham D, Humblet Y, Siena S, Khayat D, Bleiberg H, Santoro A, Bets D, Mueser M, Harstrick A, Verslype C, Chau I, Van Cutsem E. Cetuximab monotherapy and cetuximab plus irinotecan in irinotecan-refractory metastatic colorectal cancer. N Engl J Med. 2004; 351:337–345. [PubMed: 15269313]
36. Vermorken JB, Mesia R, Rivera F, Remenar E, Kawecki A, Rottey S, Erfan J, Zabolotnyy D, Kienzer H-R, Cupissol D, Peyrade F, Benasso M, Vynnychenko I, De Raucourt D, Bokemeyer C, Schueler A, Amellal N, Hitt R. Platinum-Based Chemotherapy plus Cetuximab in Head and Neck Cancer. New England Journal of Medicine. 2008; 359:1116–1127. [PubMed: 18784101]
37. Koon HK, Chan PS, Wong RN, Wu ZG, Lung ML, Chang CK, Mak NK. Targeted inhibition of the EGFR pathways enhances Zn-BC-AM PDT-induced apoptosis in well-differentiated nasopharyngeal carcinoma cells. J Cell Biochem. 2009; 108:1356–1363. [PubMed: 19816982]
38. Bhuvaneswari R, Gan YY, Soo KC, Olivo M. Targeting EGFR with photodynamic therapy in combination with Erbitux enhances in vivo bladder tumor response. Mol Cancer. 2009; 8:94. [PubMed: 19878607]
39. van Dongen GA, Visser GW, Vrouenraets MB. Photosensitizer-antibody conjugates for detection and therapy of cancer. Adv Drug Deliv Rev. 2004; 56:31–52. [PubMed: 14706444]
40. Jain RK. Normalization of tumor vasculature: an emerging concept in antiangiogenic therapy. Science. 2005; 307:58–62. [PubMed: 15637262]
41. Kessel D, Luo Y, Mathieu P, Reiners JJ Jr. Determinants of the apoptotic response to lysosomal photodamage. Photochem Photobiol. 2000; 71:196–200. [PubMed: 10687394]
42. Berg K, Moan J. Lysosomes and microtubules as targets for photochemotherapy of cancer. Photochem Photobiol. 1997; 65:403–409. [PubMed: 9077120]

43. Tibbles LA, Woodgett JR. The stress-activated protein kinase pathways. Cell Mol Life Sci. 1999; 55:1230–1254. [PubMed: 10487205]
44. Gille H, Downward J. Multiple ras effector pathways contribute to G(1) cell cycle progression. J Biol Chem. 1999; 274:22033–22040. [PubMed: 10419529]
45. Fan Z, Lu Y, Wu X, Mendelsohn J. Antibody-induced epidermal growth factor receptor dimerization mediates inhibition of autocrine proliferation of A431 squamous carcinoma cells. J Biol Chem. 1994; 269:27595–27602. [PubMed: 7961676]
46. Peng D, Fan Z, Lu Y, DeBlasio T, Scher H, Mendelsohn J. Anti-epidermal growth factor receptor monoclonal antibody 225 up-regulates p27KIP1 and induces G1 arrest in prostatic cancer cell line DU145. Cancer Res. 1996; 56:3666–3669. [PubMed: 8706005]
47. Bonni A, Brunet A, West AE, Datta SR, Takasu MA, Greenberg ME. Cell survival promoted by the Ras-MAPK signaling pathway by transcription-dependent and - independent mechanisms. Science. 1999; 286:1358–1362. [PubMed: 10558990]
48. Cross TG, Scheel-Toellner D, Henriquez NV, Deacon E, Salmon M, Lord JM. Serine/threonine protein kinases and apoptosis. Exp Cell Res. 2000; 256:34–41. [PubMed: 10739649]
49. Hayakawa J, Ohmichi M, Kurachi H, Kanda Y, Hisamoto K, Nishio Y, Adachi K, Tasaka K, Kanzaki T, Murata Y. Inhibition of BAD phosphorylation either at serine 112 via extracellular signal-regulated protein kinase cascade or at serine 136 via Akt cascade sensitizes human ovarian cancer cells to cisplatin. Cancer Res. 2000; 60:5988–5994. [PubMed: 11085518]
50. Ahmad N, Kalka K, Mukhtar H. In vitro and in vivo inhibition of epidermal growth factor receptor-tyrosine kinase pathway by photodynamic therapy. Oncogene. 2001; 20:2314–2317. [PubMed: 11402326]
51. Del Governatore M, Hamblin MR, Shea CR, Rizvi I, Molpus KG, Tanabe KK, Hasan T. Experimental photoimmunotherapy of hepatic metastases of colorectal cancer with a 17.1A chlorin(e6) immunoconjugate. Cancer Res. 2000; 60:4200–4205. [PubMed: 10945630]
52. Serebrovskaya EO, Edelweiss EF, Stremovskiy OA, Lukyanov KA, Chudakov DM, Deyev SM. Targeting cancer cells by using an antireceptor antibody-photosensitizer fusion protein. Proc Natl Acad Sci U S A. 2009; 106:9221–9225. [PubMed: 19458251]
53. Bhatti M, Yahioglu G, Milgrom LR, Garcia-Maya M, Chester KA, Deonarain MP. Targeted photodynamic therapy with multiply-loaded recombinant antibody fragments. Int J Cancer. 2008; 122:1155–1163. [PubMed: 17973256]
54. Vrouenraets MB, Visser GW, Loup C, Meunier B, Stigter M, Oppelaar H, Stewart FA, Snow GB, van Dongen GA. Targeting of a hydrophilic photosensitizer by use of internalizing monoclonal antibodies: A new possibility for use in photodynamic therapy. Int J Cancer. 2000; 88:108–114. [PubMed: 10962447]
55. Zhong W, Celli JP, Rizvi I, Mai Z, Spring BQ, Yun SH, Hasan T. In vivo high-resolution fluorescence microendoscopy for ovarian cancer detection and treatment monitoring. Br J Cancer. 2009
56. Juarranz A, Jaen P, Sanz-Rodriguez F, Cuevas J, Gonzalez S. Photodynamic therapy of cancer. Basic principles and applications. Clin Transl Oncol. 2008; 10:148–154. [PubMed: 18321817]
57. Beck TJ, Kreth FW, Beyer W, Mehrkens JH, Obermeier A, Stepp H, Stummer W, Baumgartner R. Interstitial photodynamic therapy of nonresectable malignant glioma recurrences using 5-aminolevulinic acid induced protoporphyrin IX. Lasers Surg Med. 2007; 39:386–393. [PubMed: 17565715]
58. Stepp H, Beck T, Pongratz T, Meinel T, Kreth FW, Tonn J, Stummer W. ALA and malignant glioma: fluorescence-guided resection and photodynamic treatment. J Environ Pathol Toxicol Oncol. 2007; 26:157–164. [PubMed: 17725542]
59. Savellano MD, Hasan T. Targeting cells that overexpress the epidermal growth factor receptor with polyethylene glycolated BPD verteporfin photosensitizer immunoconjugates. Photochem Photobiol. 2003; 77:431–439. [PubMed: 12733655]

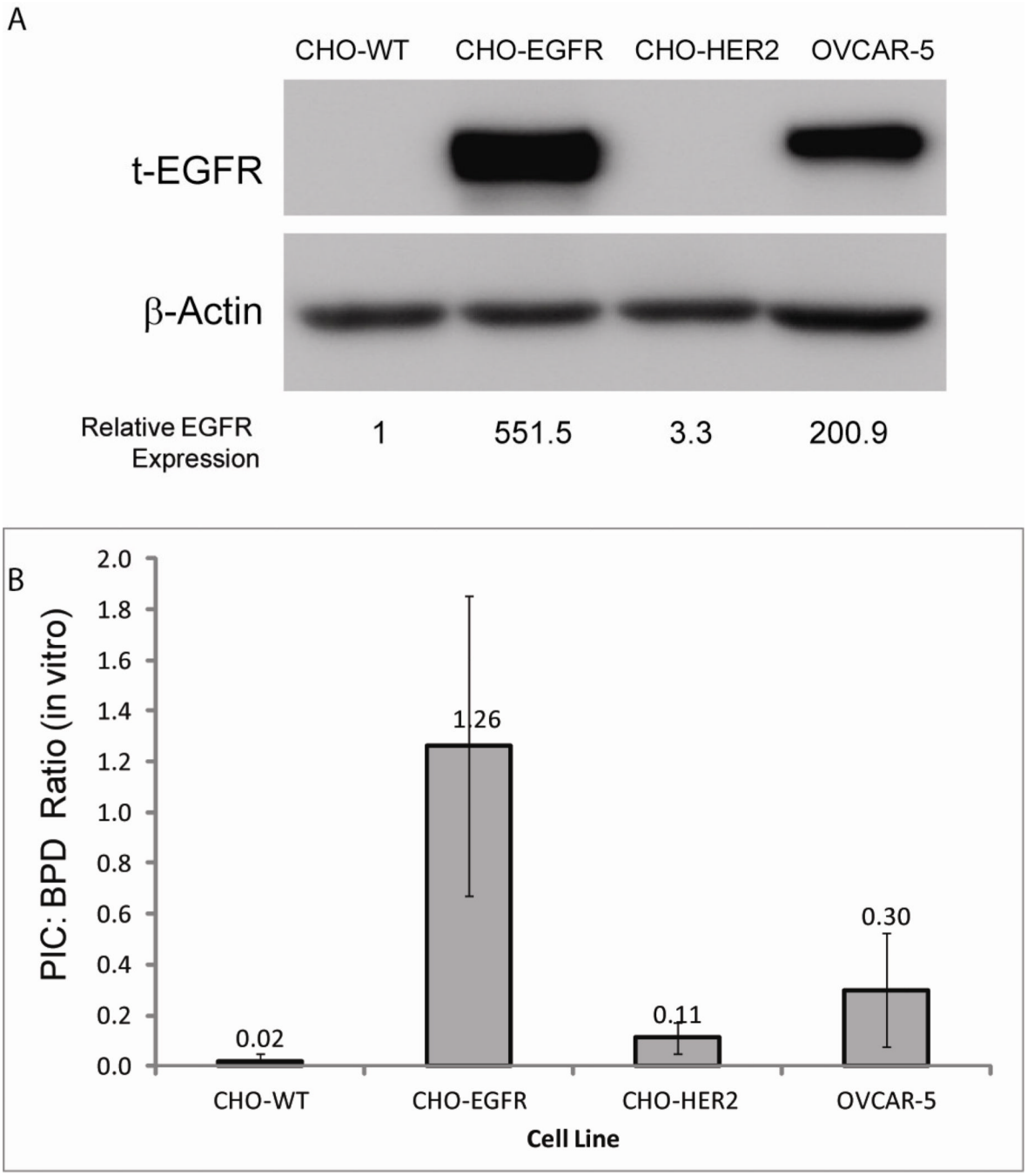

Figure 1. BPD-cetuximab PIC selectively binds to cells expressing EGFR

A) Representative western blot of whole cell lysates obtained from CHO cells stably transfected with control vector (WT), EGFR, or HER2 and OVCAR-5 ovarian cancer cells. Blots were probed with anti-EGFR antibody and anti-beta-actin to demonstrate equal loading of each sample. Densitometric analysis of EGFR expression level normalized to beta-actin loading control is indicated below each lane. **B)** Relative BPD binding in cell lines with different expression levels of EGFR: The ratio of BPD-cetuximab PIC extracted from cells to BPD extracted from cells is shown (a: $p < 0.01$ as compared to CHO-WT cells,

b: $p < 0.01$ as compared to CHO-HER2 cells; the BPD-cetuximab:BPD ratio was not statistically significant different between CHO-EGFR cells and OVCAR-5 ($p = 0.07$))

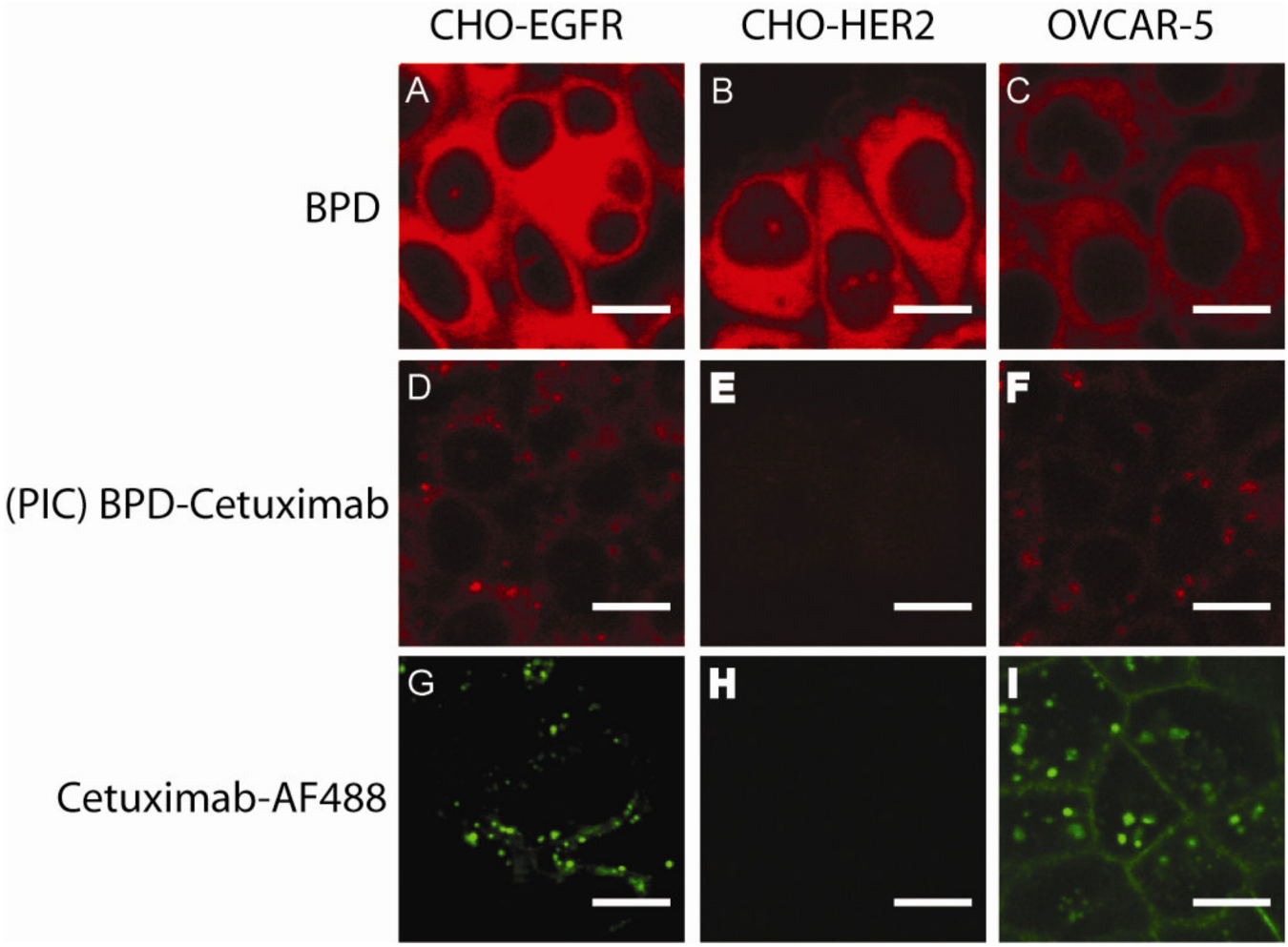

Figure 2. BPD-cetuximab PIC formulation improves selective delivery of BPD

In OVCAR-5, CHO-EGFR and CHO-HER2 cells, fluorescence was imaged using confocal microscopy to demonstrate the lack of selectivity for BPD (A, B, and C) compared to the high selectivity for the BPD-cetuximab PIC (D, E, and F) and Alexa Fluor 488 labeled parent antibody cetuximab (G, H, and I). Cells were incubated for 40 hours with 250 nM BPD or 250 nM BPD-cetuximab, fixed in 4% formalin, washed in PBS and directly visualized as described in Materials and Methods. All images were acquired using the same laser intensities to excite BPD and AF488 fluorescence followed by uniform processing using ImageJ software.

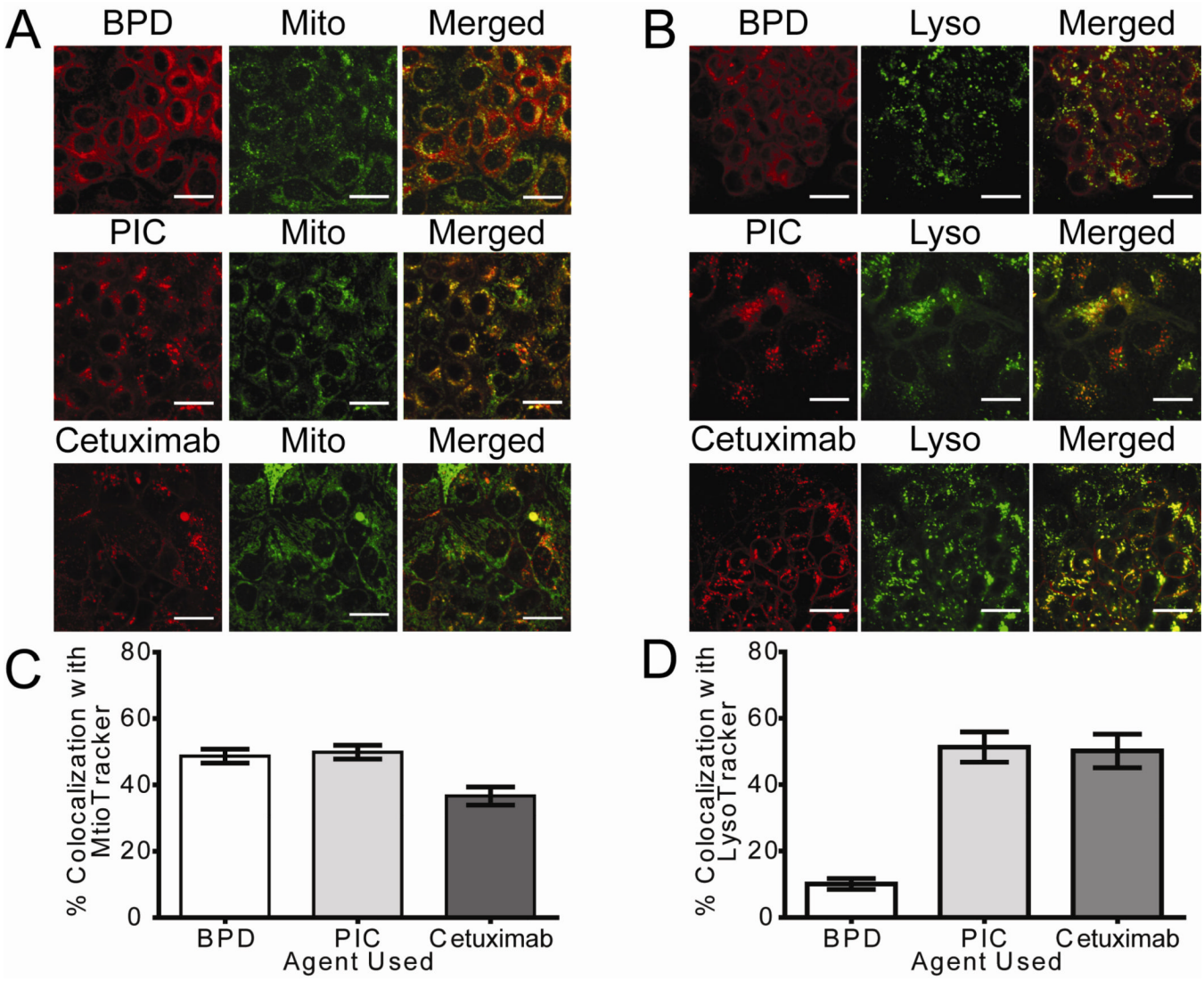

Figure 3. Cellular localization of BPD is altered by conjugation to cetuximab

Confocal fluorescence images show the subcellular localization of BPD and PIC in EGFR expressing OVCAR-5 cells. (A) Cells were incubated for 40 h with 250 nM BPD equivalents using BPD or BPD-cetuximab PIC, or 37 nM cetuximab labeled with Alexa Fluor 647 (shown in red). During the final hour of incubation (A) 100 nM MitoTracker (pseudocolored Green) or (B) 100 nM LysoTracker (pseudocolored Green) was added to the media to stain the respective organelles. The BPD fluorescence pattern is more mitochondrial, whereas cells incubated with either PIC or cetuximab show a more distinct granular distribution, which mostly colocalizes with LysoTracker suggesting lysosomal accumulation of these agents. Images are representative of multiple z-stack images acquired per condition on more than three independent experiments. Image acquisition parameters and post-processing in ImageJ was similar for all images. Scale bar =25 μm. Colocalization percentages were calculated using custom Matlab routines and are shown as the percent of colocalization with either (C) MitoTracker or (D) LysoTracker ± SEM.

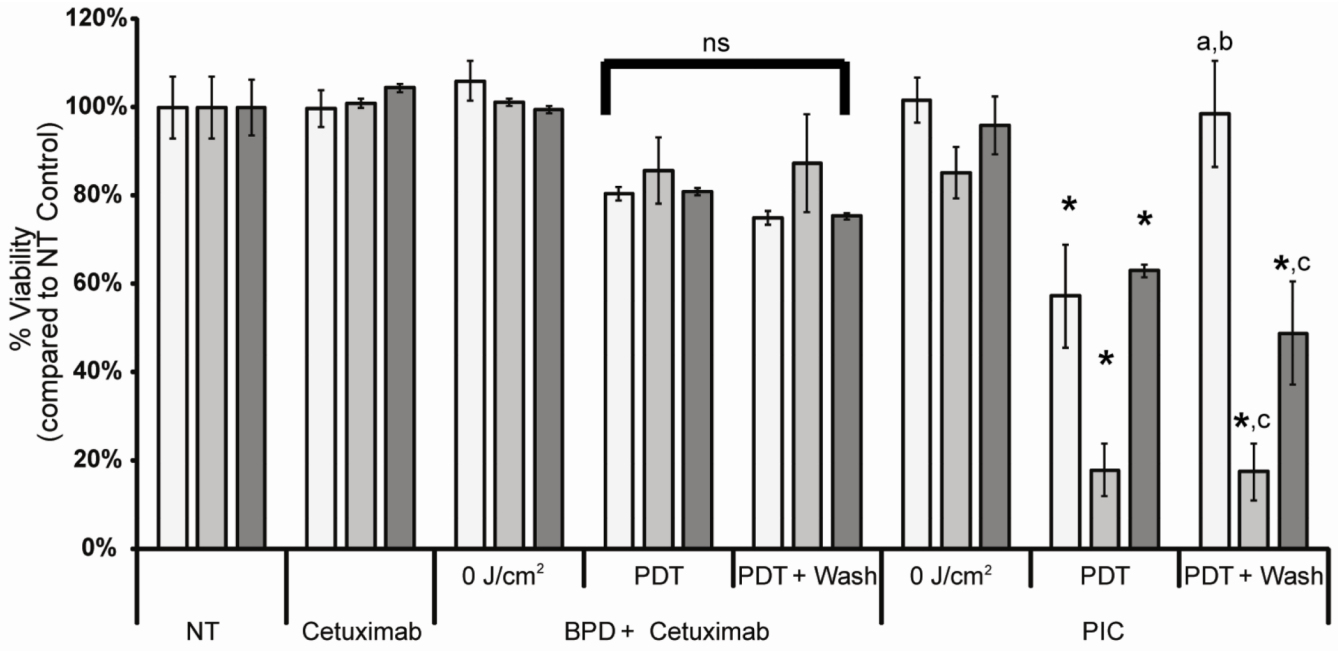

Figure 4. BPD-cetuximab selective binding results in selective phototoxicity

Viability of CHO-HER2 (open bars), CHO-EGFR (grey bars) and OVCAR-5 cells (black bars) as measured by the MTT assay. Cells were incubated with 250 nM BPD, and/or 37 nM cetuximab equivalent or PIC as indicated. After incubation, cells were illuminated with increasing doses of red light (690 nm, 40 mW/cm^2). To remove loosely bound BPD or BPD-cetuximab PIC, cells were washed with complete culture medium before illumination (PDT + wash). MTT assay was performed 24 h after illumination. The results shown represent the average of three experiments performed in triplicate each time ± standard deviation. * $p<0.05$ in student's t-test compared to agent in the absence of PDT. [a] $p<0.05$ in student's t-test compared to no treatment controls for that respective cell line. [b] $p<0.05$ in student's t-test compared to PDT without washing. [c] $p>0.05$ in student's t-test as compared to PDT without washing.

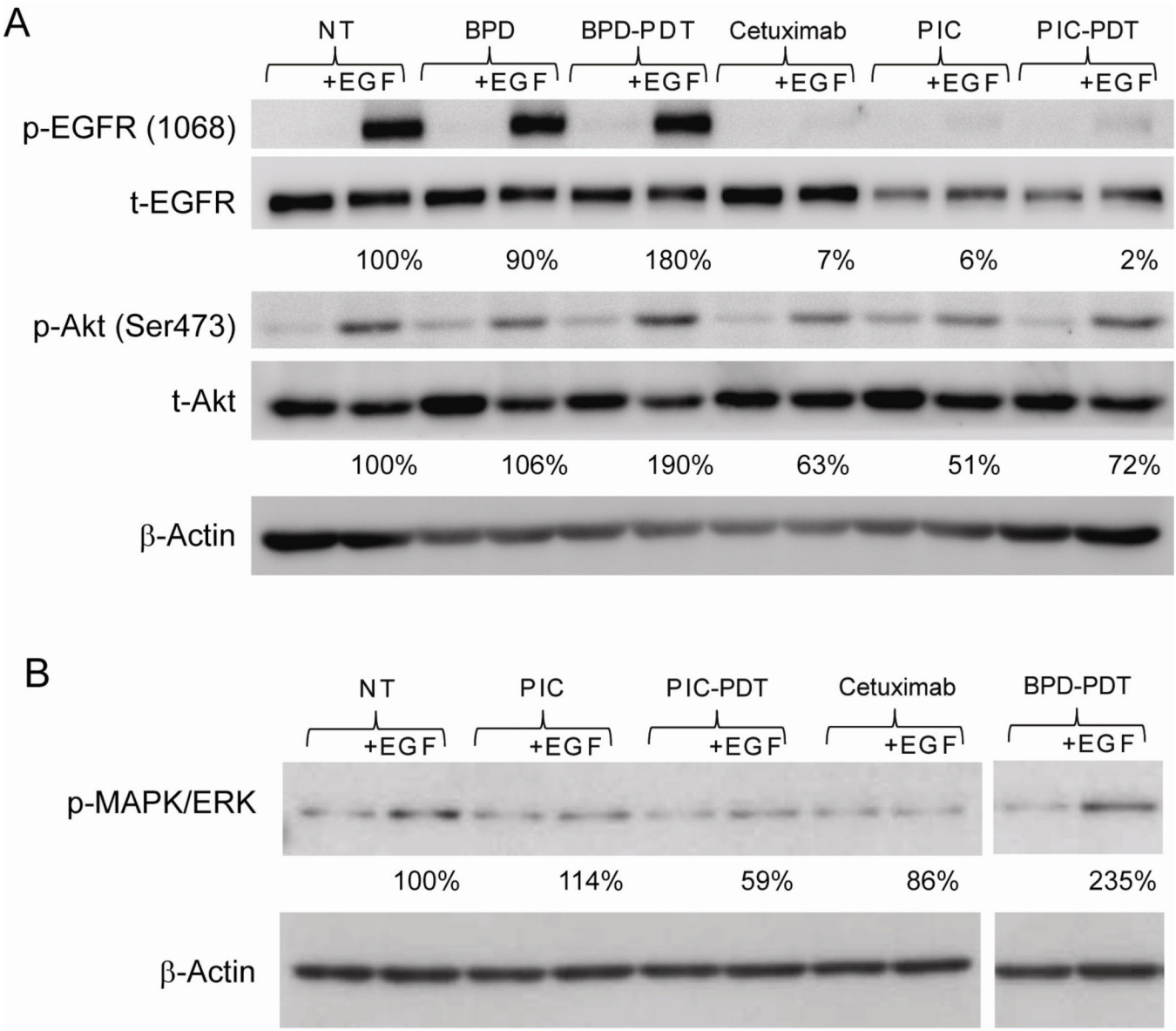

Figure 5. The presence of cetuximab alone or as part of the PIC formulation inhibits EGFR mediated signaling pathways

OVCAR-5 cells were incubated for 40 hrs with 250 nM BPD or 250 nM BPD-cetuximab (37nM cetuximab equivalent). After incubation, cells were illuminated with a dose of red light (690 nm, 40 mW/cm^2), which in earlier experiments had been shown to induce a 50% decrease in the MTT assay after 24 hrs. Cells marked cetuximab were incubated for 40 hrs with 37 nM cetuximab. Prior to lysis and sample collection, cells were incubated for 15 min with 10 ng/ml EGF. Incubation with EGF stimulated EGFR phosphorylation and Akt (A) as well as MAPK/ERK phosphorylation (B) 24 hrs after PDT. Numbers below the various lanes indicate the average increase in phosphorylation compared to no treatment (NT) controls in 3 independent experiments.